

Sub-Doppler supersonic jet spectra of the coupled $6a_0^1$ and $6b_0^1$ vibronic bands of the $S_1(^1B_{2u}) \leftarrow S_0(^1A_{1g})$ transition in monodeuterobenzene and their rovibrational analysis

By EBERHARD RIEDLE†

Institut für Physikalische und Theoretische Chemie, TU München
Lichtenbergstraße 4, D-85747 Garching, Germany and Joint Institute for
Laboratory Astrophysics, National Institute of Standards and Technology
and University of Colorado, Boulder, Colorado, 80309, USA

ANDREAS BEIL, DAVID LUCKHAUS and MARTIN QUACK
Laboratorium für Physikalische Chemie der ETH Zürich (Zentrum)
CH-8092 Zürich, Switzerland

(Received 29 April 1993; accepted 3 June 1993)

We report the rotationally resolved spectra of C_6H_5D obtained in a supersonic seeded jet by Doppler free UV laser spectroscopy with an effective resolution of about 0.0045 cm^{-1} . The coupled $6a_0^1$ and $6b_0^1$ vibronic transitions are analysed in terms of their spectroscopic constants ($\tilde{\nu}_0 = 38\,634.2429\text{ cm}^{-1}$ for $6a_0^1$ and $\tilde{\nu}_0 = 38\,637.1792\text{ cm}^{-1}$ for $6b_0^1$) and the Coriolis coupling constant $\xi_6^c = 0.095\,85\text{ cm}^{-1}$, obtained by constraining the C rotational constants to be equal for $6a^1$ and $6b^1$. Simulations of the spectra result in rotational temperatures of about 2 K. The polarizations of the two transitions could be determined unambiguously as well as the approximate ratio of the transition moments.

1. Introduction

Benzene has been a prototype molecule for numerous spectroscopic investigations [1-38]. The UV transition from the electronic ground state ($^1A_{1g}$ in D_{6h}) to the first excited singlet ($^1B_{2u}$ in D_{6h}) is electronically forbidden, but becomes vibronically allowed with the ν_6 (E_{2g}) fundamental providing the prominent 'false' origin of the electronic transition (6_0^1) with progressions in the totally symmetric fundamental ν_1 (A_{1g}) and hot band sequences with ν_{16} (E_{2u}) in the room temperature spectrum (all in Wilson's numbering scheme, see [1, 2, 29]). When replacing one hydrogen by a substituent, such as F, CH_3 or NH_2 [31, 38], the transition becomes electronically allowed (1B_2 for S_1). Then, typically, the totally symmetric component of ν_6 ($6a$, A_1 in C_{2v}) forms additional progressions on the true, allowed 0_0^0 origin ([38] shows pictures of the vibrational modes).

Substitution of hydrogen by deuterium [26] or ^{12}C by ^{13}C [29] results in an intermediate situation. In the Born-Oppenheimer approximation the electronic transition would be still forbidden, but to higher order the 0_0^0 band might become weakly allowed, the CD bond being slightly shorter than the CH bond on the

† 1991-1992 JILA Visiting Fellow. Present address: Max-Born Institut für Nichtlineare Optik und Kurzzeit spektroskopie, Rudower Chaussee 6, D-12489 Berlin, Germany.

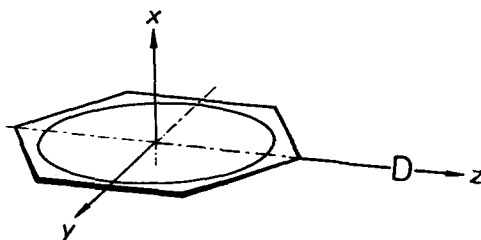


Figure 1. Structure and axis definitions for C_6H_5D .

average. Still, the most strongly allowed transitions are expected to arise from ν_6 , which in C_{2v} is split into ν_{6a} (A_1) and ν_{6b} (B_2 , following Mulliken's proposals for axis definitions, z towards the substituent, x perpendicular to the ring, B_2 being anti-symmetric with respect to the σ_{xz} plane, figure 1). However, the vibrational symmetry is rather heavily broken, as we shall see, with a shift of about 3 cm^{-1} of the B_2 fundamental towards higher wave-numbers, about 0.5% of the ν_6 fundamental wave-number.

Although there have been previous investigations of the electronic spectrum of C_6H_5D [32–35], a rotational analysis has been presented so far only for the 14_0^1 transition [32]. However, C_6H_5D is particularly suited for such an analysis, as accurate ground state rotational constants for C_6H_5D are known from microwave spectroscopy [26], in agreement with, but more accurate than the corresponding most recent structural data from Fourier transform infrared (FTIR) and laser spectroscopy [29, 30] for C_6H_6 . Previous infrared and Raman studies of C_6H_5D fundamentals do not seem to include the ν_6 fundamentals in any detail [36, and references cited therein].

The goal of the present paper is to provide an interpretation of the rovibrational line structure of the $6a_0^1$ and $6b_0^1$ bands in C_6H_5D . This analysis provides accurate excited state rovibrational constants, the interesting Coriolis coupling between the two bands and the intensity and polarization of the two transitions. We note that $6b_0^1$ in C_6H_5X electronic spectra in general appears only weakly, whereas the totally symmetric vibration $6a$ builds strong progressions. On the other hand in C_6H_5D , $6b_0^1$ appears strongly. The resulting questions of the relative intensity and polarization of the coupled bands are of interest also in relation to the corresponding bands appearing in electronic spectra of rare gas van der Waals complexes with C_6H_6 , where in C_{2v} symmetry similar effects would be expected. To our knowledge, there has been no previous rovibrational analysis to answer these questions in any of those cases.

2. Experimental

To obtain a rotationally resolved electronic spectrum of C_6H_5D , sub-Doppler resolution is necessary. In addition, reasonably strong rotational cooling will facilitate the assignment of the spectrum by reducing the number of observed lines. Both effects can be attained in the Garching spectrometer which combines a well collimated supersonic molecular beam with an extremely narrow band tunable UV laser [48, 49]. The UV light of about 130 MHz bandwidth is generated by pulsed amplification of the continuous wave (c.w.) output of a single mode dye laser (Coherent CR 699/21; Coumarin 102 dye) pumped by a Kr^+ ion laser (Coherent CR 3000 K) and subsequent frequency doubling in a BBO crystal. The UV light

needed to pump the three stages of amplification (Coumarin 500 dye) is supplied by one of the discharge tubes of a Lambda Physik EMG 150 XeCl excimer laser. This laser system delivers about 400 μJ of UV light, however, only on the order of 1 μJ (focused to about 1 mm) was used for the recording of the spectra reported here. This is necessary to avoid saturation of the stronger rovibronic transitions [48].

Excitation of the molecules to be studied can either be monitored by observation of the fluorescence emission [48] or by ionization of the electronically excited molecules by photons from a second UV laser (pumped by the second discharge tube of the excimer laser) and subsequent detection of the molecular ions in a linear time of flight mass spectrometer [49]. The latter method was used for the present study since it allows for the selection of ions of a specific mass and therefore the discrimination of other isotopomers of benzene or molecular clusters which might be present in the expansion. 100 μJ of UV light with a wavelength of 2739 \AA were used to ensure a high detection sensitivity and the two laser beams were carefully overlapped. The particular ionization wavelength was chosen as it does not generate any ions of $\text{C}_6\text{H}_5\text{D}$ by itself.

Commercially obtained $\text{C}_6\text{H}_5\text{D}$ was used after three freeze, pump and thaw cycles to prepare a premix of 42 mbar of $\text{C}_6\text{H}_5\text{D}$ and 5 bar of Ar. Due to the mass selective detection scheme used, even large impurities in the sample would not lead to extra lines in the spectrum. The gas mixture was then expanded through a pulsed valve to form the molecular beam. Before entering the interaction chamber, the beam was skimmed to reduce the residual Doppler broadening. Six individual scans of 1.6 cm^{-1} in the UV were recorded to cover the entire spectral region of interest. For absolute calibration with an accuracy of about $3 \times 10^{-3} \text{ cm}^{-1}$ the well known absorption spectrum of I_2 [50] was used. Relative calibration of the experimental spectra was performed according to the simultaneously recorded transmission spectrum of a precisely calibrated and carefully stabilized Fabry–Perot interferometer [48]. The overlapping individual scans were finally merged to the comprehensive spectrum which was digitally smoothed as described in [40]. Due to the complex nature of the recording process, relative line intensities in the spectrum might be only accurate to about 10%.

3. Analysis of the spectrum

Figure 1 shows the definition of the axis system used for monosubstituted benzene derivatives following the Mulliken convention [31, 35]. This convention is most commonly used for electronic spectra of benzene derivatives, but differs from the one often used in infrared spectroscopy [29, 36] and also the one used in [32]. In the two conventions the species B_1 and B_2 need to be interchanged. For definiteness and in order to avoid confusion we give the character table for C_{2v} in table 1 with the definition used here including the cartesian components of the electric dipole moment vector μ in the molecule fixed axis system and the components of the rotational angular momentum \mathbf{J} . Table 1 also contains the reduction n_{Γ_v} of vibrational species in C_{2v} for $\text{C}_6\text{H}_5\text{D}$ [31, 38] and the correlation with the character table for the molecular symmetry group S_2^* ($= \text{M}_{s4}$) of order four for the simultaneous permutations of carbons and protons in positions 2,3 and 5,6 respectively, i.e. $(\alpha\beta) = (26)(35)(2'6')(3'5')$, and space inversion in the centre of mass, relevant for deriving the reduction of nuclear spin symmetry species n_{Γ_s} in the molecular symmetry group. Because of a slight error concerning the nuclear spin

Table 1. Symmetry species^(a) in C_{2v} and S_2^* .

C_{2v}	S_2^*	E	C_2 ($\alpha\beta$)	σ_{xz} ($\alpha\beta$) [*]	σ_{yz} E^*	μ	\mathbf{J}	$K_a K_c$	n_{Γ_v}	n_{Γ_s}	g
A_1	A^+	1	1	1	1	μ_z		ee	11	60	60
A_2	A^-	1	1	-1	-1		J_z	eo	3	0	60
B_1	B^-	1	-1	1	-1	μ_x	J_y	oo	6	0	36
B_2	B^+	1	-1	-1	1	μ_y	J_x	oe	10	36	36

^(a) For the molecular symmetry group [41] we use the symbol S_2^* corresponding to the permutation of the units α and β consisting of several nuclei, parity of the species is indicated by + or - in the exponent, following [42] (see also text). The columns μ and \mathbf{J} indicate the species of the components of the dipole and angular momentum vectors in the molecule fixed axis system. The column $K_a K_c$ gives the combination (even, odd), which results in the rotational species indicated, n_{Γ_v} and n_{Γ_s} give the reduction of vibrational normal mode species and nuclear spin species and g gives the nuclear spin statistical weight for the corresponding rovibronic species.

statistical weights in [32], we give here a brief statement concerning the origin of the nuclear spin statistical weights, following, e.g. [42]. The character under ($\alpha\beta$), an even parity fermion permutation, must be 1. Thus the total Pauli-allowed species are A^+ and A^- (nurovibronic). The four protons 2,3,5,6 generate a reducible representation of the following structure, with total nuclear spin I for four protons in parenthesis: $D_R(I=2) = 5A^+$, $D_R(I=1) = 3A^+ + 6B^+$, $D_R(I=0) = 2A^+$, hence D_R (total, four protons) = $10A^+ + 6B^+$. These combine with the $2 \times 3 = 6$ spin functions of proton (4) and deuteron (1), hence D_R (total, all spins) = $60A^+ + 36B^+$. The 96 functions are all of positive parity. This gives the reduction n_{Γ_s} and the weights g in table 1.

The general electric dipole rovibronic selection rule is

- (i) parity change ($+ \leftrightarrow -$)
- (ii) conservation of nuclear spin symmetry (i.e. $A \not\leftrightarrow B$).

Figure 2 shows the scheme of the symmetry allowed, observed transitions. Rovibronic transitions to the $6a^1$ state are possible due to the component μ_y of the dipole operator and transitions to the $6b^1$ state due to the component μ_z . The resulting selection rules are $\Delta K_a = \pm 1, \dots$ and $\Delta K_c = \pm 1, \dots$ for the transitions to the $6a^1$ state and $\Delta K_a = 0, \pm 2, \dots$ and $\Delta K_c = \pm 1, \dots$ for the ones to the $6b^1$ state. Rovibronic states in the two manifolds can be coupled by Coriolis coupling due to the x component of the rotational angular momentum.

For numerical reasons we used an axis system x', y', z' for the rotational state calculations, with $x' = z, y' = -y, z' = x$, corresponding to the III^F representation of Watson's effective Hamiltonian (A reduction) with diagonal terms:

$$\hat{H}_{\text{rot}}^{\text{vv}} = A\hat{J}_{x'}^2 + B\hat{J}_{y'}^2 + C\hat{J}_{z'}^2 - \Delta_J \hat{J}^4 - \Delta_{JK} \hat{J}^2 \hat{J}_{z'}^2 - \Delta_K \hat{J}_{z'}^4 - \frac{1}{2} [\delta_J \hat{J}^2 + \delta_K \hat{J}_{z'}^2, \hat{J}_+^2 + \hat{J}_-^2]_+, \quad (1)$$

where $\hat{J}^2 = \hat{J}_{x'}^2 + \hat{J}_{y'}^2 + \hat{J}_{z'}^2$, and $\hat{J}_{\pm} = \hat{J}_{x'} \pm i \hat{J}_{y'}$, and with a first-order Coriolis coupling term

$$\hat{H}_{\text{cor}}^{\text{vv}} = i \xi_{6b6a}^c \hat{J}_{z'}'. \quad (2)$$

This was found sufficient to fit the spectrum. We used the program described in [39] to simulate and analyse the rotational line structure of the transitions. Ground state

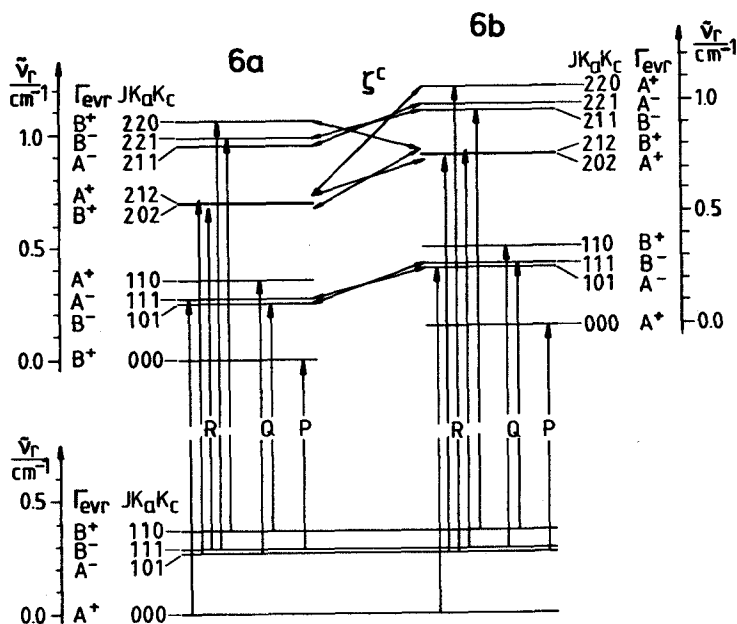


Figure 2. Scheme of the allowed rovibronic transitions of the 6a and 6b vibrations in C_6H_5D .

rotational constants were obtained from microwave spectroscopy [26]. The initial guess of the so far unknown excited state rotational constants was arbitrarily taken from the 14_0^1 transition [32] and for the Coriolis coupling constant $\xi_6^c = 2C\xi_6^c$ we used as initial guess $\zeta_6^c = 0.5788$ for the unsubstituted benzene [40]. The splitting of the vibrational frequencies 6a and 6b was estimated theoretically by Rava *et al.* [34] to be 5 cm^{-1} and, more accurately, in experiments by Rosman and Rice [33] as 3.1 cm^{-1} , which we used as starting value, together with the assumption of equal transition moments for $6a_0^1$ and $6b_0^1$. 330 assigned lines contain the large majority of stronger transitions. Including some more, weaker transitions in the fit does not change the results appreciably.

4. Results and discussion

Figure 3 shows the experimental spectrum together with the simulation using the initial guess for the spectroscopic parameters. In spite of the relatively large resolution limited linewidth of 0.0045 cm^{-1} , which may be compared to typical Doppler limited widths between 0.001 and 0.003 cm^{-1} for the fundamental transitions in the infrared at room temperature, the spectrum shows perfectly resolved rovibrational structure, because of the large changes of the moments of inertia upon electronic excitation and because of the very low temperatures of about 2 K achieved in the seeded jet expansion. This renders the assignment rather straightforward with the initial guess of a simulation systematically shifted to lower frequency with similar overall structure. One observes two moderately well separated bands. Integrating the spectrum from $38\,632.0\text{ cm}^{-1}$ to $38\,635.8\text{ cm}^{-1}$ and from $38\,635.8\text{ cm}^{-1}$ to $38\,639.2\text{ cm}^{-1}$, respectively, one finds the ratio $G_{\text{high}} : G_{\text{low}} = 1.2 \pm 0.1$ for the relative integrated band strengths of high-frequency band and low-frequency band in agreement with the value 1.3 given by Rosman and Rice [33], with $G = \int \sigma(\nu)\nu^{-1} d\nu \propto |\mu_{fi}|^2$, see [51].

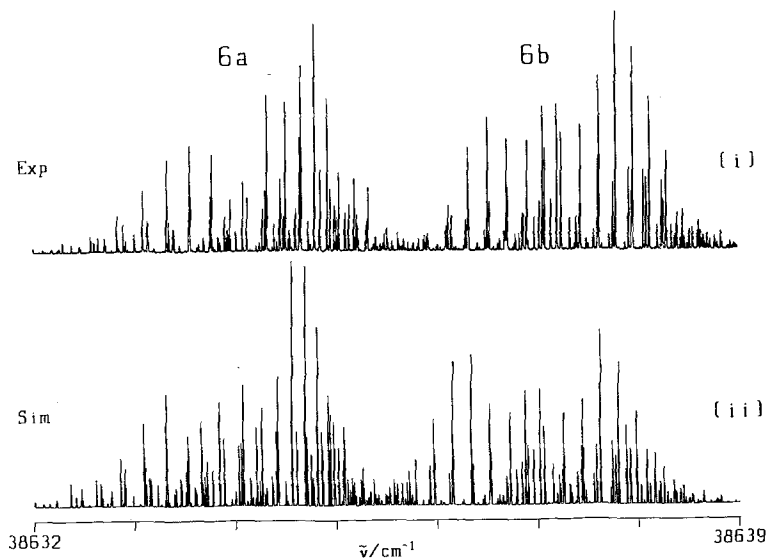


Figure 3. Upper trace (i) Experimental supersonic jet spectrum of the coupled $6a_0^1$ and $6b_0^1$ vibronic transitions of the $S_1 \leftarrow S_0$ electronic transition of C_6H_5D . The resolution is 0.0045 cm^{-1} and the estimated temperature 2 K. Lower trace (ii) Simulation of the experimental spectrum ($T_{\text{sim}} = 2\text{ K}$) with estimated spectroscopic constants (see text).

Using the automatic assignment procedure [39], we were able to assign all the rovibronic lines. Because only low J quantum numbers ($J < 6$) contribute at these very low temperatures to the spectrum, it was not possible to fit centrifugal distortion parameters. Even the two rotational constants $C(6a^1)$ and $C(6b^1)$ are highly correlated with the Coriolis coupling parameter ξ_6^c between the two levels. Within the experimental accuracy the spectra could be equally well fit with $\xi_6^c = 0$ or with $\xi_6^c = 0.09585\text{ cm}^{-1}$. However, for the fit with $\xi_6^c = 0$ the rotational constant C_{6b} ($= 0.0909\text{ cm}^{-1}$) differs much from C_{6a} ($= 0.0849\text{ cm}^{-1}$), which is not plausible for these nearly degenerate vibrations. At the same time, the large apparent inertial defects obtained from the fit ($\Delta = -6.3\text{ u}\text{\AA}^2$ for $6b^1$ and $+6.8\text{ u}\text{\AA}^2$ for $6a^1$) would contradict the known planar geometry of benzene in its S_1 state [11], see also the discussion for $6_0^1 10_0^2$ in [40]. With $\xi_6^c = 0$, furthermore, transitions involving high K_a , K_c quantum numbers also show systematic deviations, which are large compared with the root mean square deviation of the fit. Because of the limited range of J and K values accessible, we could not use these deviations for the independent determination of ξ_6^c , C_{6a} and C_{6b} . Rather, we used two constraints, firstly setting the inertial defect Δ to zero:

$$\Delta = I_c - I_a - I_b \cong 0, \quad (3)$$

or alternatively setting $C_{6a} = C_{6b}$. These physically justified constraints on the fit should provide rather accurate and reasonable values of the parameters, as summarized in table 2. The two independent fits showed no systematic deviations and provide similar parameters. More constants could be derived from unconstrained fits of spectra taken at higher temperatures, which might now easily be assigned, using the present results as a starting point.

The assignment of the low-frequency band as $6a_0^1$ (A_1 vibrational, B_2 vibronic symmetry, y polarized) and high-frequency band as $6b_0^1$ (B_2 vibrational, A_1 vibronic

Table 2. Rovibrational parameters^(a) for the vibrational ground state 0_0 (from [26]) and the excited states $6a^1$ and $6b^1$ (this work).

	fit 1			fit 2		
	0_0	$6a^1$	$6b^1$	$6a^1$	$6b^1$	$6b^1$
$\tilde{\nu}_0/\text{cm}^{-1}$	0	38634·2431(1)	38637·1794(1)	38634·2429(1)	38637·1792(1)	38637·1792(1)
A/cm^{-1}	0·189769417	0·181766(11)	0·181726(15)	0·181779(7)	0·181763(9)	0·181763(9)
B/cm^{-1}	0·177587323	0·170306(12)	0·170286(13)	0·170361(7)	0·170322(8)	0·170322(8)
C/cm^{-1}	0·091719252	0·0879247	0·0879099	0·0878886	0·0878886(16)	0·0878886(16)
$\xi_{6b,6a}^c/\text{cm}^{-1}$		0·096014(53)		0·095848(26)		
$d_{\text{rms}}/\text{cm}^{-1}$		8×10^{-4}		5×10^{-4}		
N_{data}		330		330		

^(a) Centrifugal distortion constants for 0_0 : $\Delta_{JK} = -4\cdot00277 \times 10^{-8} \text{ cm}^{-1}$; $\Delta K = -1\cdot20083 \times 10^{-7} \text{ cm}^{-1}$; $\delta_J = 6\cdot33772 \times 10^{-10} \text{ cm}^{-1}$. These were used for all states. Standard deviations are given in terms of the last digits in parentheses, fit 1 is with the constraint for the inertial defect $\Delta^{(a)} = \Delta^{(b)} = 0$, fit 2 with $C_{6a} = C_{6b}$.

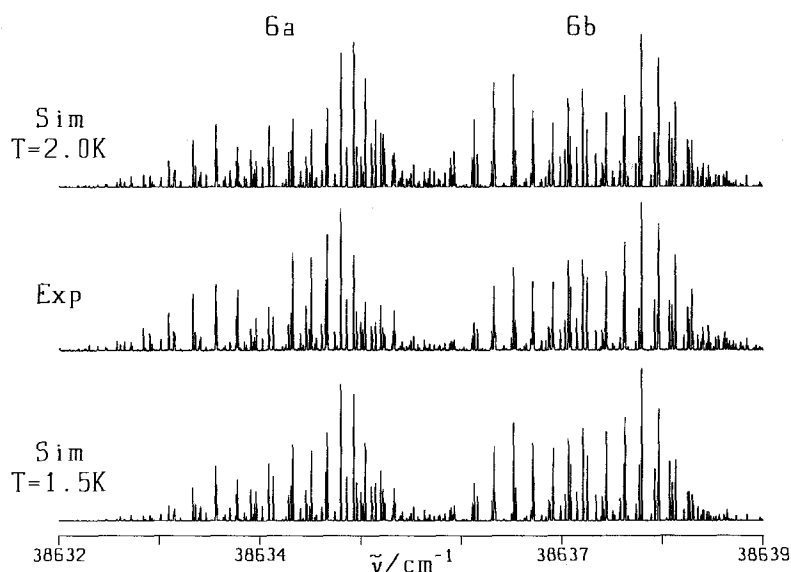


Figure 4. Experimental spectrum (see also caption figure 3) and the best simulations for $T = 2.0$ K (upper) and $T = 1.5$ K (lower).

symmetry, z polarized) results unambiguously from the present high-resolution analysis of selection rules and statistical weights for the individual line strengths. This is illustrated in figure 2. As can be seen from figure 4, the final simulations of the spectra provide an excellent agreement between experiment and simulation. The rotational temperatures for the best simulations are about 2 K. As this corresponds to $(kT/hc) > 1 \text{ cm}^{-1} \gg A \simeq B > C$, even this low temperature is somewhat too high to observe effects arising from nuclear spin symmetry conservation in the supersonic jet expansion [42, 43]. In figure 4 we also show a simulation for a rotational temperature of 1.5 K which does not show a dramatically poorer agreement with the experimental spectrum. This is partly due to the low accuracy in the line intensities caused by the complicated experimental detection. More importantly, jet conditions used in the recording of the spectrum do not provide a clean Boltzmann distribution of the rotational states [49].

In order to evaluate the ratio of transition moments (μ_a/μ_b) and the relative sign of the Coriolis coupling constant ξ_6^c with respect to the sign of this ratio, we have simulated the spectrum with variable μ_a/μ_b , using a Gaussian line shape with a full width half-maximum (FWHM) of 0.0045 cm^{-1} at various temperatures and compared with the experimental spectrum by visual inspection. The best agreement between experiment and simulation is obtained for

$$\xi_6^c \left(\frac{\mu_b}{\mu_a} \right) > 0,$$

$$\left| \frac{\mu_b}{\mu_a} \right| \cong 1.2 \pm 0.1,$$

(with T_{rot} about 2 K). One may compare this result with the degenerate polarization $|\mu_a| = |\mu_b|$ for C_6H_6 and the dominant y polarization, i.e. $|\mu_a| \gg |\mu_b|$, in monosubstituted benzene C_6H_5X with $X = \text{F}, \text{NH}_2$ etc. [37].

Assuming that the 0_0^0 transition occurs at $38\,124\text{ cm}^{-1}$ [28], one finds for the fundamentals $\nu'_{6a} = 510.2\text{ cm}^{-1}$ and $\nu'_{6b} = 513.2\text{ cm}^{-1}$, which can be compared with the theoretical predictions 513 cm^{-1} and 518 cm^{-1} by Rava *et al.* [34], based on the harmonic potential of Robey and Schlag [52]. Except for an early result [35] for the term value $6(a\text{ or }b)_1 = 603\text{ cm}^{-1}$ there seems to be no accurate knowledge of the ground state constants of 6a and 6b. Approximate hot band shifts from sequence transitions $N_0^1\ 6a, b_1^1$ are $81.5 \pm 1\text{ cm}^{-1}$ [28]. Considering the absence of anharmonicity corrections in the comparison, this shift is roughly consistent with the observed terms for $6a, b^1$ and $6a, b_1$, although the problem deserves further attention, probably best by high-resolution FTIR spectroscopy. Attempts to see 0_0^0 by 1-, 2-, and 3-photon spectroscopy directly were unsuccessful [44]. The 6a, 6b splitting in the ground state of $D_{2h}\text{-C}_6\text{H}_4\text{D}_2$ was estimated by contour analysis to be $6.6 \pm 0.3\text{ cm}^{-1}$ [45].

5. Conclusions

Supersonic jet spectra of monodeutero benzene show two prominent bands of about equal strength centred at $38\,634.24\text{ cm}^{-1}$ and $38\,637.18\text{ cm}^{-1}$, which can be unambiguously assigned due to their rotational line structure as $6a_0^1$ for the lower and $6b_0^1$ for the higher frequency. The rotational line structure is fully resolved with an experimental bandwidth of 0.0045 cm^{-1} , about an order of magnitude below the Doppler limit at room temperature. Effective rotational constants and the Coriolis coupling constant could be evaluated with good accuracy, as well as an approximate absolute value for the ratio of transition moments for the two polarizations (*y* and *z*). This ratio is close to 1 (about 1.2), which indicates the partial retainment of the symmetric, degenerate value 1 in D_{6h} benzene. In the rotational analysis it was found that the Coriolis coupling between the $6a^1$ state and the $6b^1$ state has to be included in the modelling in order to obtain physically meaningful values for the rotational constants. This off-diagonal coupling in the asymmetric top $\text{C}_6\text{H}_5\text{D}$ is the direct extension of the well known diagonal Coriolis coupling in the symmetric top C_6H_6 which splits the (*+l*) and (*-l*) levels of the 6^1 state [11, 40, 48]. The value 0.5453 for the Coriolis coupling constant calculated from $\zeta_6^C = \xi_6^C/2C$ lies at nearly 1/6 of the way between the value $\zeta_6 = 0.5788$ for C_6H_6 [40] and $\zeta_6 = 0.3912$ for C_6D_6 [49] in agreement with a simple, intuitive picture.

The line resolved rovibronic transitions allow for accurate conclusions about the rotational constants, particularly so, as Coriolis coupling is properly accounted for, and therefore confirmation of the planar D_{6h} geometry of benzene in its $^1\text{B}_{2u}$ electronic state [11, 40]. The asymmetric top $\text{C}_6\text{H}_5\text{D}$ gives, in a sense, more stringent data on this question than the symmetric top C_6H_6 . Of course, small asymmetries of the equilibrium structure so far cannot be ruled out, neither for the ground nor the excited state of benzene, as no r_e structure is known at present and even the exact planarity at equilibrium may remain subject to questions, as has been pointed out in [29], to which we refer for a critical discussion of structural data from rotationally line resolved data for benzene. In order to discuss the present rotational constants in terms of structural changes, we have performed some test calculations. A substitution structure gives $r_{\text{CH}} = 108.2\text{ pm}$ and $r_{\text{CC}} = 139.5\text{ pm}$ in the ground electronic state with D_{6h} geometry [26]. Electronic excitation (*) into the $6a^1$ or $6b^1$ levels results in a change $\Delta r_{\text{CH}} = r_{\text{CH}}^* - r_{\text{CH}} \simeq -0.5\text{ pm}$ somewhat less than indicated by the early work on benzene [11], and $\Delta r_{\text{CC}} \simeq 3.5\text{ pm}$, in essential agreement with the

early data [11]. Most of these changes result from electronic excitation, α_6^B being expected to be similar to the ground state value in C_6H_6 (about 0.00014 cm^{-1} [29]), the motion of ν_6 corresponding to a slight distortion of the CC frame [38]. Our calculations indicate that additional planar distortions of 0.1% in the CC bond length or 0.5% in r_{CH} would give significant discrepancies with our experiment on the excited electronic state, as would changes of the out of plane angle of 3° to 4° into a boat or chair form of the CC frame and 5° to 6° out of plane angle of the hydrogen atoms (with planar C_6 frame). Of course, all of these are *effective* structural changes in the excited electronic state. Very little can be said about the exact, possibly distorted r_e structure, if, for instance, there are just slight bumps in the potential at the symmetrical configuration.

The rotational analysis of the vibronic spectrum of asymmetric top benzene is also of some relevance for current discussions of the analysis of rovibronic spectra of asymmetric top complexes containing benzene [46, 47]. Assuming a rigid asymmetric arrangement of benzene in the cluster, the 6^1 state can be expected to be slightly split into its a and b components. These will again be coupled by Coriolis coupling and the influence on the rotational structure in the spectrum will be quite pronounced due to the small value of the vibronic splitting. As we have clearly shown, a meaningful structural determination will require proper inclusion of Coriolis coupling in the rotational analysis of such cluster systems.

Our work is supported financially by the Schweizerischer Nationalfonds and the Schweizerischer Schulrat, as well as by the Deutsche Forschungsgemeinschaft (experimental set up and research stipend to E.R.). We wish to thank R. Sußmann for value help with the experiments.

Appendix. List of transition wave-numbers (observed and calculated with the parameters of fit 1 in table 2). $v = 1$, ground state; $v = 2$, $6a^1$ vibronic state; $v = 3$, $6b^1$ vibronic state

v	J	K_a	K_c	$\bar{\nu}_{\text{obs}}/\text{cm}^{-1}$	$\bar{\nu}_{\text{obs}} - \bar{\nu}_{\text{calc}}/\text{cm}^{-1}$	v	J	K_a	K_c	$\bar{\nu}_{\text{obs}}/\text{cm}^{-1}$	$\bar{\nu}_{\text{obs}} - \bar{\nu}_{\text{calc}}/\text{cm}^{-1}$
2	1	1	1	38633.7766	-0.122E-04	2	4	2	2	38634.6422	0.497E-03
2	2	1	2	38633.5578	-0.838E-03	2	4	2	3	38634.7388	-0.880E-04
2	3	1	3	38633.3320	-0.577E-03	2	5	2	4	38634.8515	0.777E-04
2	4	1	4	38633.0930	-0.453E-03	2	6	2	4	38634.7598	0.833E-03
2	5	1	5	38632.8406	-0.431E-03	2	2	1	1	38634.0875	-0.137E-03
2	6	1	6	38632.5750	-0.555E-03	2	2	1	2	38633.9071	0.112E-02
2	7	1	7	38632.2964	-0.924E-03	2	3	1	3	38633.6977	0.111E-03
2	0	0	0	38633.9616	-0.111E-04	2	4	1	3	38633.6505	0.390E-04
2	1	0	1	38633.7641	0.130E-03	2	4	1	4	38633.4601	-0.666E-03
2	2	0	2	38633.5578	0.309E-03	2	5	1	4	38633.3864	-0.101E-02
2	3	0	3	38633.3320	-0.510E-03	2	5	1	5	38633.2080	-0.442E-03
2	4	0	4	38633.0930	-0.449E-03	2	6	1	5	38633.1175	-0.748E-03
2	5	0	5	38632.8406	-0.431E-03	2	6	1	6	38632.9418	-0.115E-02
2	6	0	6	38632.5750	-0.555E-03	2	3	3	0	38634.2846	0.204E-03
2	7	0	7	38632.2964	-0.924E-03	2	3	3	1	38634.4628	-0.123E-03
2	2	2	1	38633.3948	-0.695E-04	2	4	3	2	38634.5568	0.135E-03
2	4	2	3	38632.9043	-0.511E-03	2	6	3	3	38634.5662	0.107E-02
2	5	2	4	38632.6501	-0.201E-03	2	6	3	4	38634.7598	0.698E-03
2	6	2	4	38632.3824	-0.232E-03	2	3	2	1	38634.0213	0.719E-03
2	1	1	1	38633.4063	-0.658E-04	2	3	2	2	38633.8412	0.703E-04
2	1	1	0	38633.5669	0.113E-03	2	4	2	2	38633.8605	0.437E-03
2	2	1	2	38632.8572	-0.734E-03	2	4	2	3	38633.6338	0.264E-03
2	2	1	1	38633.3544	-0.206E-03	2	5	2	3	38633.5885	0.329E-03
2	3	1	3	38632.2432	-0.138E-02	2	5	2	4	38633.3864	0.104E-02
2	3	1	2	38633.1425	0.247E-03	2	6	2	5	38633.1175	-0.577E-03
2	4	1	3	38632.9043	-0.374E-04	2	4	4	0	38634.2557	0.540E-03
2	5	1	4	38632.6501	-0.171E-03	2	4	4	1	38634.4266	0.924E-03
2	6	1	5	38632.3824	-0.230E-03	2	5	4	1	38634.2490	0.102E-02
2	3	3	1	38633.0100	0.814E-04	2	6	4	2	38634.3466	0.132E-02
2	4	3	2	38632.7262	0.838E-03	2	6	4	3	38634.5714	0.131E-02
2	5	3	3	38632.4626	0.459E-03	2	4	3	1	38633.9278	0.305E-03
2	2	0	2	38632.7638	-0.453E-04	2	4	3	2	38633.7548	0.549E-03
2	2	2	1	38633.0146	-0.526E-03	2	5	3	2	38633.7930	0.169E-02
2	2	2	0	38633.1500	-0.939E-03	2	5	5	0	38634.2228	0.638E-03
2	3	2	1	38632.9241	0.996E-04	2	5	5	1	38634.3789	-0.328E-03
2	4	2	2	38632.7087	0.891E-03	2	6	5	1	38634.1618	0.168E-02
2	3	3	1	38632.6084	0.105E-03	2	5	4	1	38633.8074	0.777E-03
2	3	3	0	38632.7157	0.316E-03	2	1	1	1	38634.5095	-0.142E-03
2	4	3	1	38632.4730	0.710E-03	2	2	1	2	38634.6647	-0.358E-03
2	5	3	2	38632.2522	0.121E-03	2	3	1	3	38634.8000	-0.867E-03
2	4	4	1	38632.1832	-0.210E-03	2	4	1	4	38634.9277	-0.367E-03
2	4	4	0	38632.2621	0.289E-04	2	5	1	5	38635.0421	-0.457E-03
2	1	1	0	38634.3259	0.349E-04	2	6	1	6	38635.1433	-0.772E-03
2	2	1	1	38634.4579	0.168E-04	2	7	1	7	38635.2323	-0.582E-03
2	3	1	2	38634.6099	0.346E-03	2	8	1	8	38635.3080	-0.131E-02
2	4	1	3	38634.7388	0.347E-03	2	9	1	9	38635.3724	-0.127E-02
2	5	1	4	38634.8515	0.105E-03	2	10	1	10	38635.4225	-0.378E-02
2	1	0	1	38634.1308	-0.496E-04	2	3	3	1	38635.5662	-0.749E-06
2	2	0	2	38633.9409	-0.555E-03	2	4	3	2	38636.0242	0.234E-03
2	3	0	3	38633.7028	-0.682E-03	2	5	3	3	38636.4955	-0.673E-03
2	4	0	4	38633.4601	-0.119E-02	2	2	0	2	38634.6517	-0.105E-03
2	5	0	5	38633.2080	-0.476E-03	2	3	0	3	38634.8000	0.403E-03
2	6	0	6	38632.9418	-0.115E-02	2	4	0	4	38634.9277	-0.289E-03
2	2	2	0	38634.3087	0.151E-03	2	5	0	5	38635.0421	-0.453E-03
2	2	2	1	38634.4909	-0.853E-04	2	6	0	6	38635.1433	-0.772E-03
2	3	2	1	38634.4007	0.375E-03	2	7	0	7	38635.2323	-0.582E-03

v	J	K_a	K_c	v	J	K_a	K_c	$\bar{\nu}_{\text{obs}}/\text{cm}^{-1}$	$\bar{\nu}_{\text{obs}} - \bar{\nu}_{\text{calc}}/\text{cm}^{-1}$	v	J	K_a	K_c	v	J	K_a	K_c	$\bar{\nu}_{\text{obs}}/\text{cm}^{-1}$	$\bar{\nu}_{\text{obs}} - \bar{\nu}_{\text{calc}}/\text{cm}^{-1}$
2	8	0	8	1	7	1	7	38635.3080	-0.131E-02	3	6	0	6	1	7	0	7	38635.7289	-0.175E-03
2	9	0	9	1	8	1	8	38635.3724	-0.127E-02	3	7	0	7	1	8	0	8	38635.5228	-0.294E-02
2	10	0	10	1	9	1	9	38635.4225	-0.378E-02	3	8	0	8	1	9	0	9	38635.3185	-0.898E-03
2	2	2	1	1	1	1	0	38634.8579	0.348E-04	3	1	1	0	1	2	1	1	38636.5400	0.427E-03
2	2	2	0	1	1	1	1	38635.0189	0.181E-05	3	1	1	1	1	2	1	2	38636.7171	-0.823E-03
2	3	2	2	1	2	1	1	38634.9986	-0.139E-03	3	2	1	1	1	3	1	2	38636.3035	0.501E-03
2	3	2	1	1	2	1	2	38635.4963	-0.140E-03	3	2	1	2	1	3	1	3	38636.5191	-0.655E-03
2	4	2	3	1	3	1	2	38635.1098	-0.600E-04	3	3	1	2	1	4	1	3	38636.1039	0.472E-03
2	4	2	2	1	3	1	3	38636.0091	0.094E-03	3	3	1	3	1	4	1	4	38636.3244	-0.190E-03
2	5	2	4	1	4	1	3	38635.2189	-0.359E-03	3	4	1	3	1	5	1	4	38635.8964	0.432E-03
2	5	2	3	1	4	1	4	38636.4955	0.107E-02	3	4	1	4	1	5	1	5	38636.1277	-0.464E-03
2	6	2	5	1	5	1	4	38635.3185	0.299E-03	3	5	1	4	1	6	1	5	38635.6844	-0.121E-03
2	8	2	7	1	7	1	6	38635.4783	0.352E-03	3	5	1	5	1	6	1	6	38635.9291	-0.662E-03
2	9	2	8	1	8	1	7	38635.5382	-0.896E-03	3	6	1	5	1	7	1	6	38635.4703	-0.545E-03
2	4	4	1	1	3	1	2	38635.9022	0.200E-03	3	6	1	6	1	7	1	7	38635.7289	-0.175E-03
2	3	1	2	1	2	2	1	38634.9569	0.305E-05	3	7	1	7	1	8	1	8	38635.5228	-0.294E-02
2	4	1	3	1	3	2	2	38635.1035	0.345E-04	3	8	1	8	1	9	1	9	38635.3185	-0.898E-03
2	5	1	4	1	4	2	3	38635.2189	0.192E-03	3	1	0	1	1	2	2	0	38636.3372	-0.267E-03
2	6	1	5	1	5	2	4	38635.3185	0.335E-03	3	2	0	2	1	3	2	1	38635.8184	0.421E-03
2	8	1	7	1	7	2	6	38635.4783	0.353E-03	3	2	2	0	1	3	2	1	38636.1601	-0.503E-04
2	9	1	8	1	8	2	7	38635.5382	-0.896E-03	3	2	2	1	1	3	2	2	38636.3316	0.309E-03
2	3	3	1	1	2	2	0	38635.1959	-0.544E-04	3	3	2	1	1	4	2	2	38635.8847	0.993E-03
2	3	3	0	1	2	2	1	38635.3329	0.458E-03	3	3	2	2	1	4	2	3	38636.1089	0.334E-03
2	4	3	2	1	3	2	2	38635.3236	0.337E-03	3	4	2	2	1	5	2	3	38635.6696	-0.117E-03
2	4	3	1	1	3	2	2	38635.7829	0.777E-03	3	4	2	3	1	5	2	4	38635.8964	-0.383E-04
2	5	3	3	1	4	2	2	38635.4079	-0.281E-03	3	5	2	3	1	6	2	4	38635.4530	0.164E-02
2	5	3	2	1	4	2	3	38636.2854	0.543E-03	3	5	2	4	1	6	2	5	38635.6844	-0.153E-03
2	6	3	4	1	5	2	3	38635.4963	0.640E-04	3	6	2	5	1	7	2	6	38635.4703	-0.547E-03
2	7	3	5	1	6	2	4	38635.5789	-0.554E-05	3	7	2	6	1	8	2	7	38635.2546	-0.247E-03
2	8	3	6	1	7	2	5	38635.6494	-0.282E-03	3	2	1	2	1	3	3	1	38635.7469	0.791E-03
2	5	5	1	1	4	2	2	38636.2364	0.344E-03	3	3	1	2	1	4	3	1	38635.4225	0.712E-03
2	5	2	3	1	4	3	2	38635.3890	-0.775E-04	3	3	3	0	1	4	3	1	38635.7737	0.717E-03
2	7	2	5	1	6	3	4	38635.5789	0.176E-03	3	3	3	1	1	4	3	2	38635.9345	-0.266E-03
2	8	2	6	1	7	3	5	38635.6494	-0.269E-03	3	4	3	1	1	5	3	2	38635.4530	-0.178E-03
2	4	4	1	1	3	3	0	38635.5228	0.543E-03	3	4	3	2	1	5	3	3	38635.6844	0.258E-03
2	4	4	0	1	3	3	1	38635.6302	0.343E-03	3	5	3	2	1	6	3	3	38635.2189	0.204E-02
2	5	4	2	1	4	3	1	38635.6386	0.327E-03	3	5	3	3	1	6	3	4	38635.4530	-0.180E-03
2	5	4	1	1	4	3	2	38636.0502	0.131E-02	3	3	2	1	1	4	4	0	38635.4835	0.142E-02
2	6	4	3	1	5	3	2	38635.6989	0.869E-03	3	4	2	2	1	5	4	1	38635.0078	0.324E-03
2	5	3	2	1	4	4	1	38635.4835	0.106E-02	3	4	4	0	1	5	4	1	38635.3809	0.146E-02
2	6	3	3	1	5	4	2	38635.6553	0.954E-03	3	5	4	2	1	6	4	3	38635.2488	0.145E-02
2	7	3	4	1	6	4	3	38635.7552	0.166E-02	3	2	2	1	1	2	0	2	38637.4345	-0.688E-04
2	5	5	1	1	4	4	0	38635.8349	0.467E-03	3	3	2	2	1	3	0	3	38637.5756	-0.267E-03
2	5	5	0	1	4	4	1	38635.9139	0.608E-03	3	4	2	3	1	4	0	4	38637.7304	-0.154E-03
2	6	5	2	1	5	4	1	38635.9439	0.854E-03	3	5	2	4	1	5	0	5	38637.8857	0.232E-04
2	7	5	3	1	6	4	2	38635.9818	0.107E-02	3	6	2	5	1	6	0	6	38638.0401	0.113E-02
2	6	4	2	1	5	5	1	38635.6989	0.113E-02	3	7	2	6	1	7	0	7	38638.1901	0.138E-03
2	6	6	0	1	5	5	1	38636.1849	0.779E-03	3	1	1	1	1	1	1	0	38637.0844	-0.403E-03
2	7	7	1	1	6	6	0	38636.4092	0.143E-02	3	1	1	0	1	1	1	1	38637.2496	-0.323E-03
2	7	7	0	1	6	6	1	38636.4435	0.848E-03	3	2	1	2	1	2	1	1	38636.9031	-0.619E-03
3	0	0	0	1	1	0	1	38636.9094	-0.693E-03	3	2	1	1	1	2	1	2	38637.3986	-0.515E-03
3	1	0	1	1	2	0	2	38636.7069	-0.814E-03	3	3	1	3	1	3	1	2	38636.6948	-0.762E-03
3	2	0	2	1	3	0	3	38636.5191	0.417E-03	3	3	1	2	1	3	1	3	38637.5703	0.169E-03
3	3	0	3	1	4	0	4	38636.3244	-0.121E-03	3	4	1	4	1	4	1	4	38636.4955	-0.491E-03
3	4	0	4	1	5	0	5	38636.1277	-0.451E-03	3	4	1	3	1	4	1	4	38637.7304	0.355E-03
3	5	0	5	1	6	0	6	38635.9291	-0.662E-03	3	5	1	4	1	5	1	5	38637.8857	0.575E-04

ν J K_a K_c	ν J K_a K_c	$\tilde{\nu}_{\text{obs}}/\text{cm}^{-1}$	$\tilde{\nu}_{\text{obs}} - \tilde{\nu}_{\text{calc}}/\text{cm}^{-1}$	ν J K_a K_c	ν J K_a K_c	$\tilde{\nu}_{\text{obs}}/\text{cm}^{-1}$	$\tilde{\nu}_{\text{obs}} - \tilde{\nu}_{\text{calc}}/\text{cm}^{-1}$
3 6 1 5	1 6 1 6	38638.0401	0.113E-02	3 2 1 2	1 1 1 1	38637.6138	-0.268E-03
3 7 1 6	1 7 1 7	38638.1901	0.139E-03	3 3 1 2	1 2 1 1	38637.9542	0.105E-03
3 3 3 1	1 3 1 2	38637.4115	0.410E-03	3 3 1 3	1 2 1 2	38637.7922	0.522E-03
3 4 3 2	1 4 1 3	38637.5184	0.364E-03	3 4 1 3	1 3 1 2	38638.1008	-0.217E-03
3 5 3 3	1 5 1 4	38637.6530	-0.304E-03	3 4 1 4	1 3 1 3	38637.9624	-0.294E-03
3 6 3 4	1 6 1 5	38637.7922	-0.586E-03	3 5 1 4	1 4 1 3	38638.2526	-0.879E-03
3 2 0 2	1 2 2 1	38636.8654	-0.625E-03	3 5 1 5	1 4 1 4	38638.1301	-0.118E-02
3 3 0 3	1 3 2 2	38636.8891	-0.434E-03	3 6 1 5	1 5 1 4	38638.4056	-0.814E-03
3 4 0 4	1 4 2 3	38636.4955	0.361E-04	3 6 1 6	1 5 1 5	38638.2957	-0.189E-02
3 6 0 6	1 6 2 5	38636.0958	-0.668E-03	3 7 1 6	1 6 1 5	38638.5563	-0.106E-02
3 2 2 1	1 2 2 0	38637.0644	0.776E-04	3 7 1 7	1 6 1 6	38638.4592	-0.210E-02
3 2 2 0	1 2 2 1	38637.2082	0.345E-05	3 8 1 7	1 7 1 6	38638.7049	-0.834E-03
3 3 2 2	1 3 2 1	38636.8750	-0.164E-03	3 8 1 8	1 7 1 7	38638.6199	-0.215E-02
3 3 2 1	1 3 2 2	38637.3369	0.188E-03	3 9 1 9	1 8 1 8	38638.7774	-0.207E-02
3 4 2 3	1 4 2 2	38636.6420	-0.562E-03	3 3 3 0	1 2 1 1	38638.3051	-0.190E-03
3 4 2 2	1 4 2 3	38637.5015	0.480E-03	3 3 3 1	1 2 1 2	38638.5073	0.939E-04
3 5 2 4	1 5 2 3	38636.4215	-0.187E-03	3 4 3 1	1 3 1 2	38638.7303	-0.109E-03
3 5 2 3	1 5 2 4	38637.6530	0.173E-02	3 4 3 2	1 3 1 3	38638.9844	-0.340E-03
3 6 2 5	1 6 2 4	38636.2063	-0.165E-03	3 5 3 2	1 4 1 3	38639.2453	0.123E-02
3 6 2 4	1 6 2 5	38637.7922	-0.415E-03	3 3 2 1	1 2 2 0	38638.0700	0.257E-03
3 7 2 5	1 7 2 6	38637.9322	0.134E-02	3 3 2 2	1 2 2 1	38637.9234	0.190E-03
3 4 4 1	1 4 4 2	38637.3855	0.396E-03	3 4 2 2	1 3 2 1	38638.2675	-0.118E-03
3 5 4 2	1 5 2 3	38637.4498	0.971E-03	3 4 2 3	1 3 2 2	38638.0955	-0.663E-04
3 3 1 2	1 3 3 1	38636.7961	-0.385E-03	3 5 2 3	1 4 2 2	38638.3972	-0.196E-03
3 4 1 3	1 4 3 2	38636.6243	-0.393E-03	3 5 2 4	1 4 2 3	38638.2526	-0.390E-03
3 3 3 1	1 3 3 0	38637.0316	0.253E-03	3 6 2 4	1 5 2 3	38638.5286	-0.115E-02
3 3 3 0	1 3 3 1	38637.1478	0.120E-03	3 6 2 5	1 5 2 4	38638.4056	-0.782E-03
3 4 3 2	1 4 3 1	38636.8363	-0.965E-04	3 7 2 5	1 6 2 4	38638.6664	-0.780E-04
3 5 3 3	1 5 3 2	38636.5820	0.878E-03	3 7 2 6	1 6 2 5	38638.5563	-0.105E-02
3 5 3 2	1 5 3 3	38637.4115	0.132E-02	3 8 2 6	1 7 2 5	38638.8018	-0.147E-03
3 5 2 3	1 5 4 2	38636.5400	-0.568E-03	3 8 2 7	1 7 2 6	38638.7049	-0.834E-03
3 4 4 1	1 4 4 0	38636.9840	0.520E-03	3 4 4 0	1 3 2 1	38638.6399	0.322E-03
3 4 4 0	1 4 4 1	38637.0712	0.634E-03	3 4 4 1	1 3 2 2	38638.8379	-0.208E-03
3 5 4 2	1 5 4 1	38636.7871	0.512E-03	3 5 4 1	1 4 2 2	38639.0097	0.916E-03
3 5 4 1	1 5 4 2	38637.1527	0.744E-03	3 5 4 2	1 4 2 3	38639.2813	0.117E-02
3 5 5 1	1 5 5 0	38636.9195	0.111E-02	3 6 4 2	1 5 2 3	38639.4993	0.123E-02
3 6 5 1	1 6 5 2	38637.0316	0.109E-03	3 4 3 1	1 3 3 0	38638.3505	-0.166E-03
3 6 6 1	1 6 6 0	38636.8363	0.169E-02	3 4 3 2	1 3 3 1	38638.2112	0.106E-03
3 6 6 0	1 6 6 1	38636.8750	0.907E-03	3 5 3 2	1 4 3 1	38638.5627	0.266E-03
3 1 0 1	1 0 0 0	38637.4404	-0.344E-03	3 5 3 3	1 4 3 2	38638.3822	0.172E-03
3 2 0 2	1 1 0 1	38637.6249	-0.203E-03	3 6 3 3	1 5 3 2	38638.6837	0.840E-03
3 3 0 3	1 2 0 2	38637.7922	-0.612E-03	3 6 3 4	1 5 3 3	38638.5286	0.750E-03
3 4 0 4	1 3 0 3	38637.9624	-0.365E-03	3 7 3 4	1 6 3 3	38638.7928	0.317E-03
3 5 0 5	1 4 0 4	38638.1301	-0.119E-02	3 7 3 5	1 6 3 4	38638.6664	0.829E-04
3 6 0 6	1 5 0 5	38638.2957	-0.189E-02	3 5 5 0	1 4 3 1	38638.9735	0.146E-02
3 7 0 7	1 6 0 6	38638.4592	-0.210E-02	3 6 5 1	1 5 3 2	38639.2813	0.172E-02
3 8 0 8	1 7 0 7	38638.6199	-0.215E-02	3 5 4 1	1 4 4 0	38638.6078	0.639E-03
3 9 0 9	1 8 0 8	38638.7774	-0.207E-02	3 5 4 2	1 4 4 1	38638.4783	0.583E-03
3 2 2 0	1 1 0 1	38637.9672	-0.744E-04	3 6 4 2	1 5 4 1	38638.8379	0.208E-02
3 3 2 1	1 2 0 2	38638.4399	-0.895E-04	3 6 4 3	1 5 4 2	38638.6504	0.227E-03
3 4 2 2	1 3 0 3	38638.9687	0.379E-03	3 7 4 3	1 6 4 2	38638.9573	0.584E-03
3 5 2 3	1 4 0 4	38639.4860	0.612E-03	3 7 4 4	1 6 4 3	38638.7878	0.787E-03
3 2 1 1	1 1 1 0	38637.7659	-0.945E-04	3 6 5 2	1 5 5 1	38638.7245	0.135E-02

References

- [1] WILSON, E. B., 1934, *Phys. Rev.*, **45**, 706.
- [2] HERZBERG, G., 1945, *Molecular Spectra and Molecular Structure*, Vol. II (van Nostrand); 1966, *Ibid.*, Vol. III.
- [3] WILSON, E. B., DECIUS, J. C., and CROSS, P. C., 1955, *Molecular Vibrations* (New York: McGraw-Hill).
- [4] RUMPF, K., and MECKE, R., 1939, *Z. phys. Chem. B*, **44**, 299.
- [5] HENRY, B. R., and SIEBRAND, W., 1968, *J. chem. Phys.*, **49**, 5369; HAYWARD, R. J., HENRY, B. R., and SIEBRAND, W., 1973, *J. molec. Spectrosc.*, **46**, 207.
- [6] KISTIAKOWSKY, G. B., and PARMENTER, C. S., 1965, *J. chem. Phys.*, **42**, 2942.
- [7] BIXON, M., and JORTNER, J., 1968, *J. chem. Phys.*, **48**, 715.
- [8] STOCKBURGER, M., 1968, *Ber. Bunsenges. phys. Chem.*, **72**, 151.
- [9] PARMENTER, C. S., and SCHUYLER, M. W., 1970, *J. chem. Phys.*, **52**, 5366.
- [10] KEMPER, H. F., and STOCKBURGER, M., 1970, *J. chem. Phys.*, **53**, 268.
- [11] CALLOMON, J. H., DUNN, T. M., and MILLS, I. M., 1966, *Phil. Trans. R. Soc., Lond. A*, **259**, 499, and references therein.
- [12] SCHUBERT, U., RIEDLE, E., and NEUSSER, H. J., 1989, *J. chem. Phys.*, **90**, 5994; SCHUBERT, U., RIEDLE, E., NEUSSER, H. J., and SCHLAG, E. W., 1986, *Ibid.*, **84**, 6182, and reference therein.
- [13] BURBERRY, M. S., and ALBRECHT, A. C., 1979, *J. chem. Phys.*, **70**, 147.
- [14] BRAY, R. G., and BERRY, M. J., 1979, *J. chem. Phys.*, **71**, 4909.
- [15] QUACK, M., 1983, *Energy Storage and Redistribution in Molecules*, edited by J. Hinze (New York: Plenum), p. 493.
- [16] PAGE, R. H., SHEN, Y. R., and LEE, Y. T., 1988, *J. chem. Phys.*, **88**, 4621, and references therein.
- [17] CABANA, A., BACHAND, J., and GIGUÈRE, J., 1974, *Can. J. Phys.*, **52**, 1949.
- [18] KAUPPINEN, J., JENSEN, P., and BRODERSEN, S., 1980, *J. molec. Spectrosc.*, **83**, 161.
- [19] LINDENMAYER, J., MAGG, U., and JONES, H., 1988, *J. molec. Spectrosc.*, **128**, 172.
- [20] PLIVA, J., and PINE, A. S., 1982, *J. molec. Spectrosc.*, **93**, 209.
- [21] PLIVA, J., and JOHNS, J. W. C., 1983, *Can. J. Phys.*, **61**, 269.
- [22] PLIVA, J., and JOHNS, J. W. C., 1984, *J. molec. Spectrosc.*, **107**, 318.
- [23] JENSEN, H. B., and BRODERSEN, S., 1979, *J. Raman Spectrosc.*, **8**, 103.
- [24] HOLLINGER, A. B., and WELSH, H. L., 1978, *Can. J. Phys.*, **56**, 974.
- [25] ACKER, W. P., LEACH, D. H., and CHANG, R. K., 1989, *Chem. Phys. Lett.*, **155**, 491.
- [26] OLDANI, M., and BAUDER, A., 1984, *Chem. Phys. Lett.*, **108**, 7.
- [27] OZKABAK, A. G., GOODMAN, L., and WIBERG, K. B., 1990, *J. chem. Phys.*, **92**, 4115.
- [28] SUR, A., KNEE, J., and JOHNSON, P. M., 1982, *J. chem. Phys.*, **77**, 654.
- [29] HOLLNSTEIN, H., PICCIRILLO, S., QUACK, M., and SNELS, M., 1990, *Molec. Phys.*, **71**, 759.
- [30] JUNTILLA, M. L., DOMENECH, J. L., FRASER, G. T., and PINE, A. S., 1991, *J. molec. Spectrosc.*, **147**, 513.
- [31] QUACK, M., and STOCKBURGER, M., 1972, *J. molec. Spectrosc.*, **43**, 87.
- [32] BRUNO, A., RIEDLE, E., and NEUSSER, H. J., 1986, *Chem. Phys. Lett.*, **126**, 558.
- [33] ROSMAN, R. L., and RICE, S. A., 1986, *Chem. Phys. Lett.*, **132**, 351.
- [34] RAVA, R. P., PHILIS, J. G., KROGH-JESPERSEN, K., and GOODMAN, L., 1983, *J. chem. Phys.*, **79**, 4664.
- [35] GARFORTH, F. M., INGOLD, C. K., and POOLE, H. G., 1948, *J. Chem. Soc. (Lond.)*, 406.
- [36] THAKUR, S. N., GOODMAN, L., and OZKABAK, A. G., 1986, *J. chem. Phys.*, **84**, 6642.
- [37] HOLLAS, J. M., 1982, *High Resolution Spectroscopy* (London: Butterworths), chap. 6.
- [38] FUSON, N., GARRIGOU-LAGRANGE, C., and JOSIEN, M. L., 1960, *Spectrochim. Acta*, **16**, 106.
- [39] LUCKHAUS, D., and QUACK, M., 1989, *Molec. Phys.*, **68**, 745; 1991, *Chem. Phys. Lett.*, **180**, 524.
- [40] RIEDLE, E., and PLIVA, J., 1991, *Chem. Phys.*, **152**, 375. (This paper still used old, superseded ground state rotational constants for C₆H₆, see [29] for the previously published, new data, recently confirmed [30].)
- [41] LONGUET-HIGGINS, H. C., 1963, *Molec. Phys.*, **6**, 445.
- [42] QUACK, M., 1977, *Molec. Phys.*, **34**, 477.

- [43] AMREIN, A., QUACK, M., and SCHMITT, U., 1988, *J. phys. Chem.*, **92**, 5455.
- [44] GOODMAN, L., 1992, private communication.
- [45] GOODMAN, L., and NIBU, Y., 1988, *Chem. Phys. Letters*, **143**, 551.
- [46] SCHMIDT, M., MONS, M., LE CALVÉ, J., MILLIE, P., and COSSART-MAGOS, C., 1991, *Chem. Phys. Letters*, **183**, 69.
- [47] GOTCH, A. J., and ZWIER, T. S., 1992, *J. chem. Phys.*, **96**, 3388.
- [48] RIEDLE, E., KNITTEL, Th., WEBER, Th., and NEUSSER, H. J., 1989, *J. chem. Phys.*, **91**, 4555.
- [49] WEBER, Th., VON BARGEN, A., RIEDLE, E., and NEUSSER, H. J., 1990, *J. chem. Phys.*, **92**, 90.
- [50] GERSTENKORN, S., and LUC, P., 1978, *Atlas du Spectre d'Absorption de la Molecule de l'Iode* (Paris: CNRS); a correction of -0.0056 cm^{-1} was used according to GERSTENKORN, S., and LUC, P., 1979, *Rev. Phys. Appl.*, **14**, 791.
- [51] QUACK, M., 1990, *Ann. Rev. Phys. Chem.*, **41**, 839.
- [52] ROBNEY, M. J., and SCHLAG, E. W., 1977, *J. chem. Phys.*, **67**, 2775.